Supporting Information

A fluorescent probe for rapid detection of thiols and Imaging of thiols reducing repair and H_2O_2 oxidative stress cycles in living cells

Zhangrong Lou[†] , Peng Li[†], Xiaofei Sun, Songqiu Yang, Bingshuai Wang and Keli Han*

State Key Laboratory of Molecular Reaction Dynamics, Dalian Institute of Chemical Physics (DICP), Chinese Academy of Sciences (CAS), 457 Zhongshan Road, Dalian 116023, P. R. China
E-mail: klhan@dicp.ac.cn

Contents:

[†]Both authors contribute equally to this work.

1. General Experimental Section

Materials and characterization: Common reagents or materials were obtained from commercial source of analytical reagent grade, and used without further purification except as otherwise noted. The $ONOO^-$ source was the donor 3-Morpholinosydnonimine hydrochloride (SIN-1, 50.0 μmol/ml)[1]. NO is generated in form of 3-(Aminopropyl)-1-hydroxy-3-isopropyl-2-oxo-1-triazene (NOC-5). $^1O_2$ was generated by the reaction of H_2O_2 with NaOCl[2] and $O_2^{-}\cdot$ was created by KO_2[3]. ·OH was generated by Fenton reaction between Fe^{II}(EDTA) and H_2O_2 quantitively, and Fe^{II}(EDTA) concentrations represented ·OH concentrations[4]. Tert-butylhydroperoxide (t-BuOOH) and cumene hydroperoxide (CuOOH) could also use to induce ROS in biological systems[5]. Hypochlorous acid (HOCl) was standardized ($\varepsilon_{292\ nm}$= 350 $M^{-1}cm^{-1}$)[6]. Ultrapure water was used throughout the analytical experiments. ^{1}H NMR, ^{13}C NMR and ^{77}Se NMR spectra were obtained on a Bruker DRX-400 spectrometer, and the ^{1}H NMR and ^{13}C NMR chemical shifts (δ) are reported in ppm relative to TMS (Me_4Si) as internal reference.

Absorption and fluorescence analysis: Steady-state UV/Vis spectra were measured at room temperature on a Lambda 35 UV-visible Spectrophotometer (Perkin-Elmer) with 1.0-cm glass cells. Fluorescence emission spectra were obtained at room temperature on a Fluoromax-4 Spectrofluorometer (Horiba-Jobin Yvon), with a Xenon lamp and 1.0-cm quartz cells. With a pipette gun (Eppendorf), taking 40 μL of the probe FSeSeF (Ethanol, 0.5 mM) and then the solution was diluted to 2.0 μM with 10ml 20 mM PB buffers before measurement. The concentration of FSeSeF was 2.0 μM throughout the analysis experiments except that otherwise pointed out. The fluorescence intensity was measured with the excitation wavelength 490 nm except as otherwise noted, and the excitation and emission slits were set to 1 and 1 nm, respectively.

Kinetic assays: The kinetic measurement of the reaction of FSeSeF (1.0 μM) with different concentrations of GSH was carried out on an Applied Photophysics SX.18MV stopped-flow spectrophotometer in a single-mixing mode of the instrument with 10:1 (v/v) ratio at 25 ^{o}C. The time dependence of the fluorescent response of FSeSeF at 514 nm to GSH was determined in sodium phosphate buffer (50 mM, 7.40) with the excitation wavelength 488 nm. The spectra changes of the reaction were monitored at time interval of 0.50 ms.

Cell culture and confocal imaging: HeLa cells were seeded at a density of 1×10^6 cells mL^{-1} for confocal imaging in RPMI 1640 Medium supplemented with 15% fetal bovine serum (FBS), $NaHCO_3$ (2 g/L), and 1% antibiotics (penicillin /streptomycin, 100 U/ml). Cultures were maintained at 37 °C under a humidified atmosphere containing 5% CO_2. The cells were subcultured by scraping and seeding on 35 mm × 12 mm glass bottom cell culture dishes according to the instructions from the manufacturer. Florescent images were acquired on a FV1000 confocal laser-scanning microscope (Olympus) with an objective lens (×10, ×40, ×60, ×100). The excitation wavelength was set to 405 nm (Figure 3g), 488 nm. Prior to imaging, the medium was removed. Cell imaging was carried out after washing cells with physiological saline (0.9 %) for three times.

MTT Assay: HeLa cells (10^6 cell mL^{-1}) were dispersed within replicate 96-well microtiter plates to a total volume of 200 μL $well^{-1}$. Plates were maintained at 37 °C in a 5% CO_2/95% air incubator for 4 h. HeLa cells were then incubated for 24 h upon

different concentrations probe of 10^{-4}, 10^{-5}, 10^{-6}, 10^{-7} and 10^{-8} M respectively. MTT (Sigma) solution (5.0 mg mL^{-1}, PBS) was then added to each well. After 4 h, the remaining MTT solution was removed, and 200 μL of DMSO was added to each well to dissolve the formazan crystals. Absorbance was measured at 570 nm in a TRITURUS microplate reader. Calculation of IC50 values was done according to Huber and Koella[7].

2. Synthesis and Characterization of Compounds

The general synthetic route of the probe FSeSeF was described in Scheme S1.

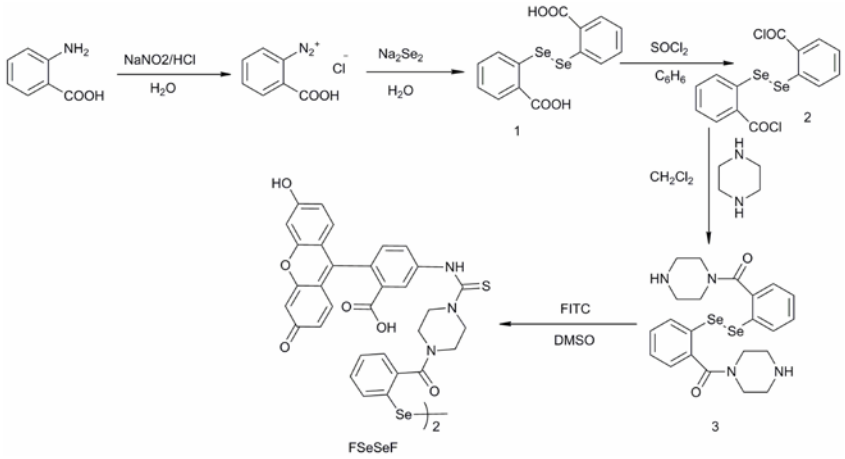

Scheme S1. The synthesis of FSeSeF.

Synthesis of 2,2'-diselanediyldibenzoic acid (1): Under the N_2 atmosphere, to a three-neck flask containing 35 ml water suspended with 5.10 g (0.065 mol) elemental selenium was dropped 4.45 g (0.130 mol) $NaBH_4$ aqueous solution. After the selenium was dissolved, another 5.13 g (0.065 mol) of selenium was added in portions. Then the mixture was stirred and heated for 30 minutes to ensure the selenium was dissolved completely. The generated brownish red solution was alkalified with 25 ml 10 mol/L NaOH aqueous solution[9]. After the solution was cooled to 5 °C with ice bath, diazonium salt synthesized from 18.00 g (0.130 mol) of anthranilic acid was added in drops at a rate to maintain the temperature of reaction mixture below 10 °C. Finally, the subsequent mixture was stirred for 3 h at 60 °C and additionally 3h at room temperature. The mixture was acidified with hydrochloric acid to make the pH 3~4, and then filtered. The brownish precipitate was washed thoroughly with water and dissolved with Na_2CO_3 aqueous solution once again. Solid impurities were filtered and the brownish red filtrates were acidified with hydrochloric acid to pH < 1. The generated light yellow precipitate was filtered and neutralized thoroughly with water. Recrystallization from acetic acid followed by washing with acetic acid afforded a light yellow powder (9.86 g, 37.92%). ^{1}H NMR (400 MHz, $CDCl_3$) δ(ppm): 13.76 (br, 1H), 8.06-8.03 (m, 1H), 7.68 (m, 1H), 7.50 (m, 1H), 7.39-7.35 (m, 1H). MS (API-ES): *m/z*, Calcd for $C_{14}H_{10}O_4Se_2$: 401.9, found: $[M-H]^+$ 400.9.

Synthesis of [diselanediylbis(2,1-phenylene)] bis(piperazin-1-ylmethanone) (3): A solution in a 50 ml three-neck flask containing 0.80 g (0.002 mol) of 2,2'-diselanediyldibenzoic acid **1** and 12 ml benzene was refluxed under N_2, then 0.56 g (0.004 mol) thionyl chloride was added. The reaction was continued until diselenide **1** had dissolved completely[10,11]. After that, the benzene and thionyl chloride were

evaporated in vacuum and the residue without purifying was dissolved in 20 ml dichloromethane (CH_2Cl_2) for next step. To a mixture of 1.76 g (0.020 mol) piperazine and 20 ml CH_2Cl_2, the acquired coarse product of 2,2'-diselanediyldibenzoyl chloride **2** in CH_2Cl_2 was added dropwise for 2.5 h. After this period, the mixture was stirred at ambient temperature for another 4h. The generated yellow reaction mixture was neutralized with NaOH aqueous solution and the aqueous phase was washed with CH_2Cl_2, the CH_2Cl_2 phase was washed with water. The combined organic layers were dried over anhydrous Na_2SO_4 and then the solvent was evaporated. The obtained residue was purified on a short-column chromatography (silica gel, ethyl acetate: methanol=1:2, +2 % triethylamine). ^{1}H NMR (400 MHz, $CDCl_3$) δ(ppm): 7.74-7.72 (m, 1H), 7.23-7.13 (m, 3H), 5.23 (br, 1H), 3.69 (br, 2H), 3.27 (br, 2H), 2.80 (br, 4H). MS (API-ES): *m/z*, Calcd for $C_{22}H_{26}N_4O_2Se_2$: 538.0, found: $[M+H]^+$ 539.0.

Synthesis of 5,5'-((4,4'-(2,2'-diselanediylbis (benzoyl))bis(piperazine-1,1'- carbonothioyl)) bis (azanediyl))bis (2-(6-hydroxy-3-oxo-3H-xanthen-9-yl) benzoic acid) (FSeSeF): A solution of diselenide **3** (0.45 g, 0.836 mmol) in 5ml dimethyl sulfoxide (DMSO) that dried with $CaSO_4$ for 24 h was added at room temperature to a magnetically stirred fluorescein isothiocyanate (0.69 g, 1.774 mmol) in 20 ml DMSO. Then the reaction was continued to stir for 85 h under anhydrous atmosphere. After there was no diselenide (3) in the reaction mixture, the solvent was evaporated on a rotary evaporator and the residue was purified on a short-column chromatography (silica gel, ethyl acetate: acetic acid=50:1), an orange powder was obtained (0.20 g, 17.54%). ^{1}H NMR (400 MHz, d^6-DMSO) δ(ppm): 11.97 (br, 1H), 10.13 (s, 2H), 9.77 (s, 1H), 7.98 (d, J=2.0, 1H), 7.80-7.77 (m, 2H), 7.43-7.42 (m, 3H), 7.19 (d, J= 8.0, 1H), 6.68 (d, J=1.6, 2H), 6.58 (d, J=2.8, 3H), 4.05-4.00 (m, 4H), 3.78 (br, 2H), 3.43 (br, 2H). ^{13}C NMR (100 MHz, d^6-DMSO) δ(ppm): 181.50, 181.37, 171.88, 168.49, 167.92, 159.43, 159.26, 151.80, 147.81, 142.67, 142.54, 136.29, 131.89, 131.73, 131.63, 130.64, 129.25, 128.90, 127.51, 127.11, 126.06, 123.48, 118.86, 118.74, 112.60, 112.51, 109.70, 109.65, 102.24, 102.17, 82.96, 20.96. ^{77}Se NMR (95 MHz, d^6-DMSO) δ (ppm): 432.42. MS (API-ES): *m/z*, Calcd for $C_{64}H_{48}N_6O_{12}S_2Se_2$: 1316.1, found: $[M+H]^+$ 1317.1, $[M+Na]^+$ 1339.3, $[M–H]^-$ 1315.2. HRMS (API-ES): m/z, Calcd for $[M–H]^-$ 1315.1024, found: $[M–H]^-$ 1315.1021.

3. Photographs of FSeSeF Solution

The photographs of FSeSeF solution in the presence and absence were shown in Figure S6. Figure S6a displayed the changes in the absorption and Figure S6b demonstrated the increase of fluorescence intensity after the addition of GSH.

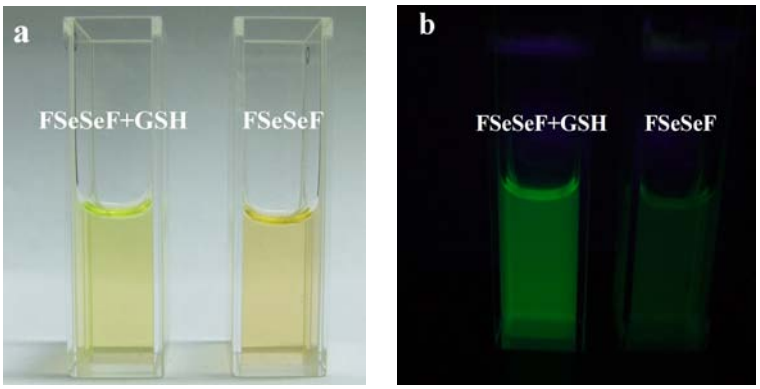

Figure S1. a) The absorption photographs of FSeSeF in the presence (Left) and absence (Right) of GSH. b) The fluorescence photographs of FSeSeF in the presence (Left) and absence (Right) of GSH with the excitation of ultraviolet lamp (365 nm).

4. Absorption and Fluorescence Titration Experiment

The changes of fluorescence intensity at 514 nm dependent on the thiols concentrations were shown in Figure S2a. A gradual increase in fluorescence intensity was observed with the addition of GSH. After adding two equivalent of GSH, there was no obvious change in fluorescence at 514 nm with the further increases of GSH concentration. However, a minor increase in fluorescence was observed again when adding 100 μM GSH. In addition, the fluorescence intensity of FSeSeF was linearly proportional to the concentration of GSH in the range from 0 to 2.0 μM, the regression equation was $F_{514\,nm}$ = 70140 × [GSH] + 116515 with a linear coefficient r = 0.964.

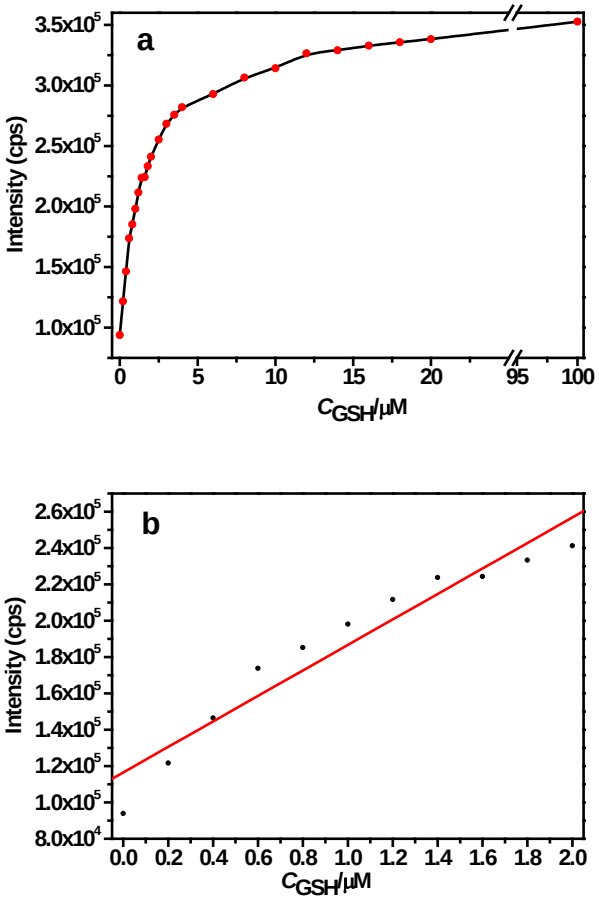

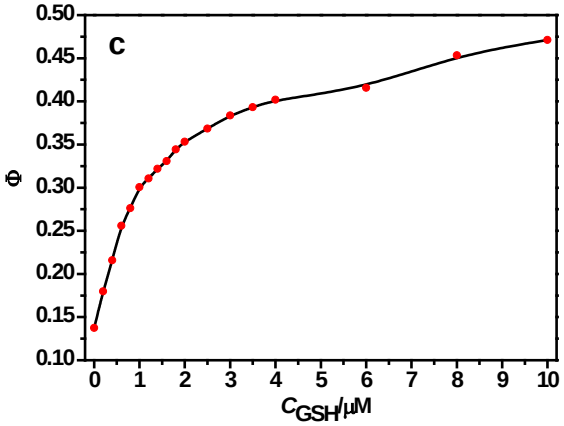

Figure S2. a) Fluorescence intensity of FSeSeF (2.0 μM) at 514 nm responding to different concentrations of GSH (0, 0.2, 0.4, 0.6, 0.8, 1.0, 1.2, 1.4, 1.6, 1.8, 2.0, 2.5, 3.0, 3.5, 4.0, 6.0, 8.0, 10.0, 12.0, 14.0, 16.0, 18.0, 20.0 and 100.0 μM). b) The relationship of the fluorescence intensity at 514 nm with the concentration of GSH in the range of 0–2.0 μM. c) The relationship of the fluorescence quantum yield with the concentration of GSH in the range of 0–10.0 μM. The excitation wavelength was set to 470 nm.

5.The calculation of detection limit

The detection limit was determined from the fluorescence titration data based on a reported method[12]. According to the result of titrating experiment, the fluorescence intensity at 514 nm were normalized between the minimum intensity and the maximum intensity. A linear regression curve was then fitted to these normalized fluorescence intensity data, and the point at which this line crossed the ordinate axis was considered as the detection limit (2.25×10^{-7} M).

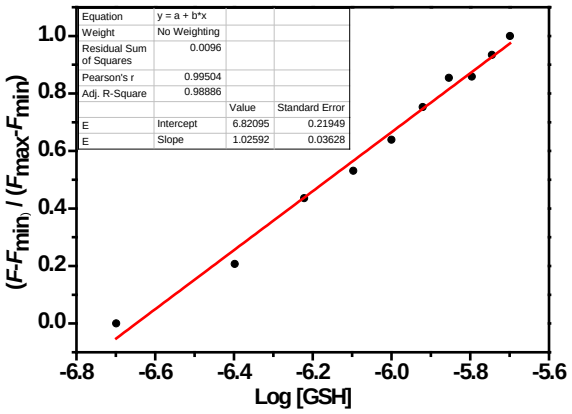

Figure S3. Normalized response of the fluorescence signal to changing GSH concentrations. Where, F_{max} was the maximum fluorescence intensity, F_{min} was the minimum fluorescence intensity, F was the fluorescence intensity at different GSH concentrations.

6. The Effects of pH values

The pH effects on the fluorescence intensity at 514 nm of FSeSeF at a concentration of 2 μM in the absecnce and presence of GSH were investigated. As shown in Figure S4, with increasing of pH values, the changing format of the intensity at 514 nm of the probe before adding GSH was the same as that after the addition of two equiv GSH. The fluorescence was quenched at low pH values while increased with the medium transferring from acidic to be neutral or alkaline. Although the change of fluorescence intensity of FSeSeF was pH-dependent, there was no obvious variation near the physiological pH, indicating the fluorescent probe was promising for biological applications.

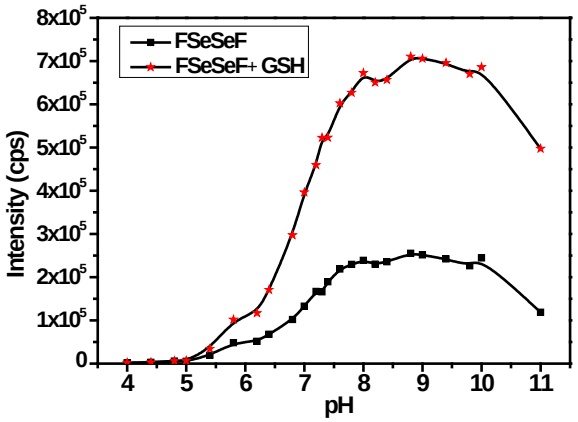

Figure S4. pH-dependent fluorescence intensity of FSeSeF at 514 nm (excited at 490 nm) in the absence (square, black) and presence (star, red) of GSH, the concentration of FSeSeF was 2.0 μM and the quantity of GSH was 4.0 μM. pH 4.0, 4.4, 4.8, 5, 5.4, 5.8, 6.2, 6.4, 6.8, 7, 7.2, 7.3, 7.4, 7.6, 7.8, 8, 8.2, 8.4, 8.8, 9, 9.4, 9.8, 10, 11.

7. Kinetic assays of FSeSeF with GSH

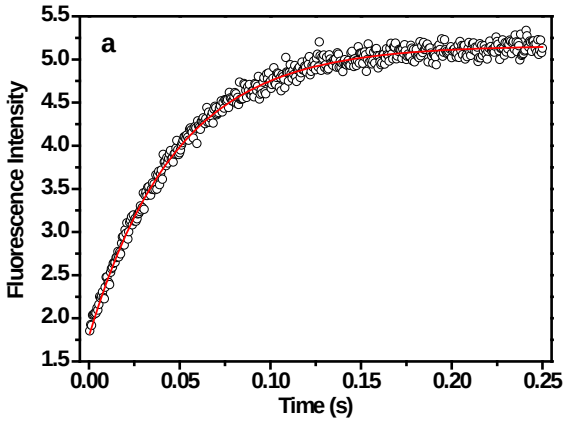

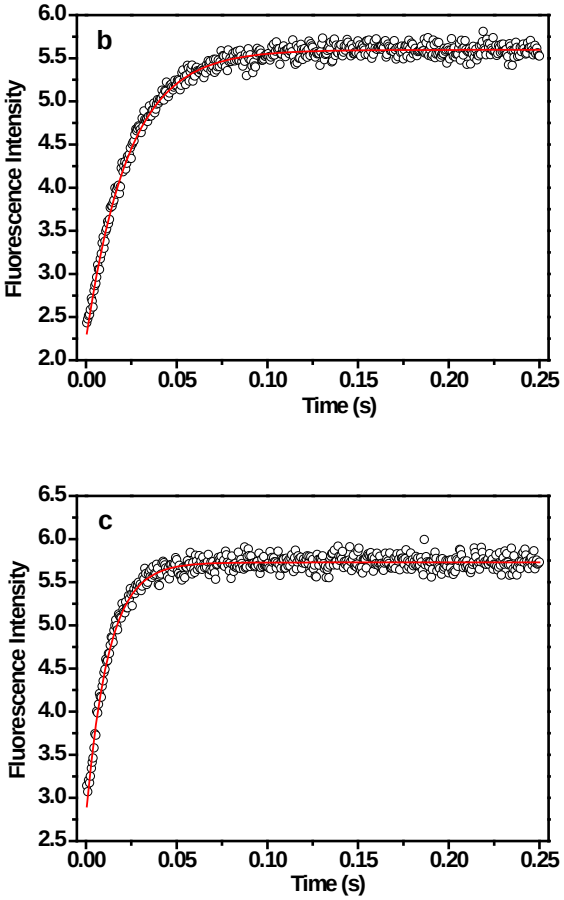

Figure S5. Time course of the fluorescent response of FSeSeF (1.0 μM) at 514 nm to different concentrations of GSH with the excitation wavelength 488 nm. a) The mixed concentration of GSH was 25 μM. b) GSH was 50 μM. c) GSH was 100 μM. The spectra changes of the reaction were monitored at time interval of 0.50 ms. The best fitting gave the observed first-order rate constant (k_{obs}) of 21.05 s^{-1}, 43.01 s^{-1}, 81.50s^{-1} for 25 μM, 50 μM and 100 μM GSH, respectively. The relevant observed second rate constant k_{obsd} was 8.4×10^5 $M^{-1}S^{-1}$, 8.6×10^5 $M^{-1}S^{-1}$, 8.1×10^5 $M^{-1}S^{-1}$. Considering the thiolate anion, the rate constant k was estimated with $k=k_{obsd}(1+10^{pKa-pH})$, with 8.75 as the microscopic pKa value of GSH[13,14,15].

The time course assay of fluorescence intensity at 514 nm for 1h before and after the addition of two equivalent of GSH was displayed in Figure S6. It can be noted that there was nearly no fluorescence changes observed within next 1 hour in the aqueous media at room temperature.

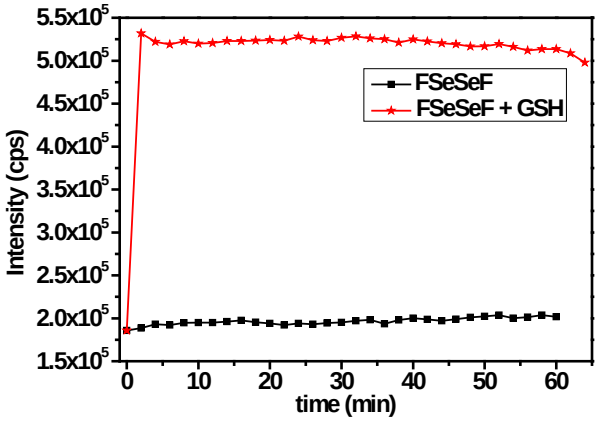

Figure S6. The changes of fluorescence intensity of FSeSeF (2.0 μM) at 514 nm depending on time before (square, black) and after (star, red) adding two equivalent of GSH.

8. Reversibility assays of FSeSeF

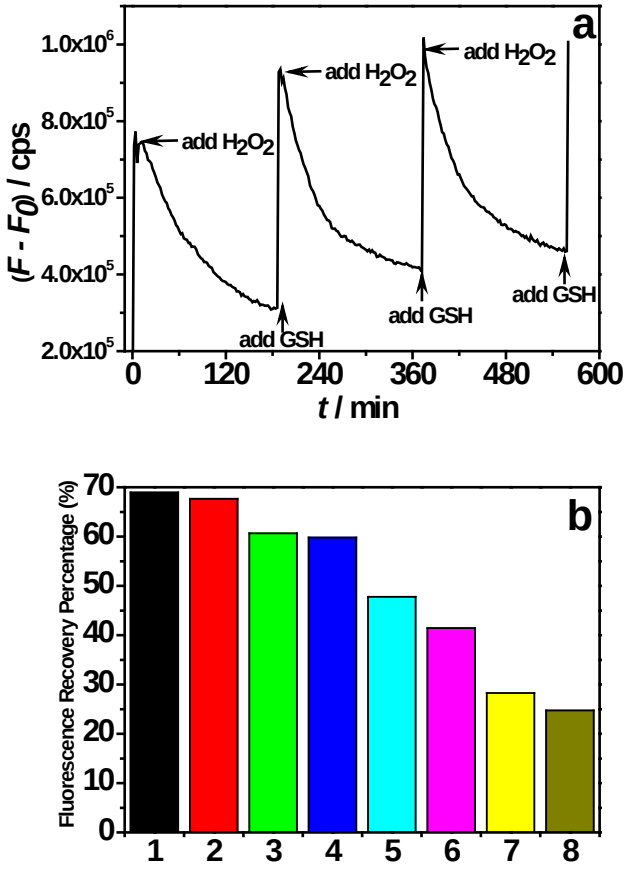

Figure S7. (a) Fluorescence responses of FSeSeF to redox cycles. A solution of 5 μM FSeSeF was treated with 10.0 μM GSH and 10.0 μM H_2O_2. (b) Fluorescence recovery rate of various ROS. FSeSeF was cloven by 2 equiv of GSH, and the solution was then treated with various ROS: 1, H_2O_2 (10.0 μM); 2, *tert*-butylhydroperoxide (10.0

μM); 3, $ONOO^-$ (10.0 μM); 4, cumene hydroperoxide (10.0 μM); 5, $^1O_2$ (10.0 μM); 6, O_2^-(10.0 μM); 7, ·OH (10.0 μM); 8, NaClO (10.0 μM). The fluorescence recovery rate (%) was calculated as follows: Fluorescence Recovery Rate = $(F_1–F)/(F_1–F_0) \times 100\%$, where, F and F_0 are the emission intensity in the presence and that in the absence of GSH, respectively. F is the fluorescence intensity of the probe after adding ROS for 3 h. All fluorescence intensities were acquired at 514 nm.

9. Additional Confocal Images

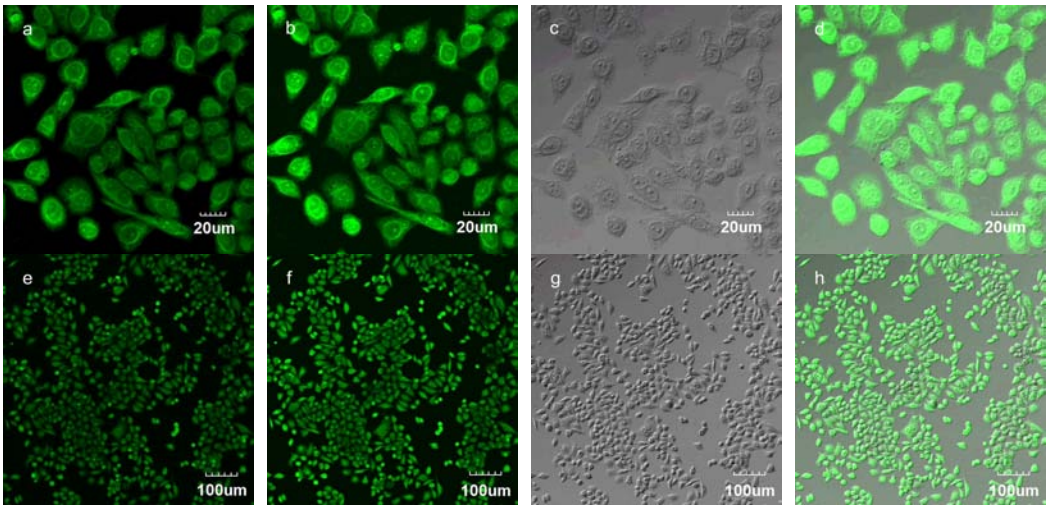

Figure S8. Confocal fluorescence images of the changes in thiol concentration. (a) Incubated with 15 μM FSeSeF for 5 min. (b) Addition of 1 mM α-lipoic acid for 30 min. (c) Bright-field image of (b). (d) The overlay of (b) and (c). Figure (e)-(h) were acquired with an objective lens (×10) that in parallel to figure (a)-(d). Scale bars represent 20 μm (a-d) and 100 μm (e-h), respectively. The images were obtained with a excitation wavelength of 488 nm and emission range of 495 to 595 nm.

10. Bright-Field Images

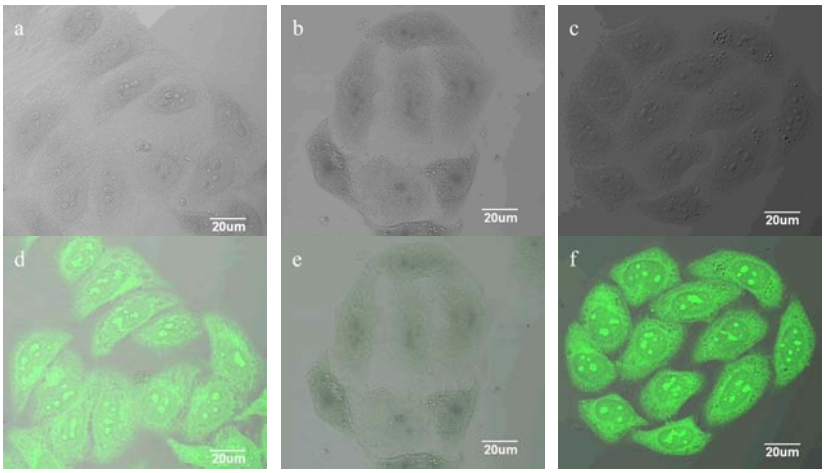

Figure S9. Bright-field images of Figure 3a–c. Image (d), (e), (f) was the overlay of Figure 3(a), (b), (c) with the image (a), (b), (c), respectively.

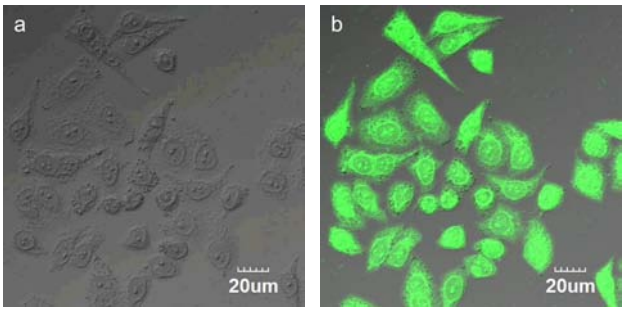

Figure S10. Bright-field images of Figure 3f. Image (b) was the overlay of Figure 3(f), with the image (a).

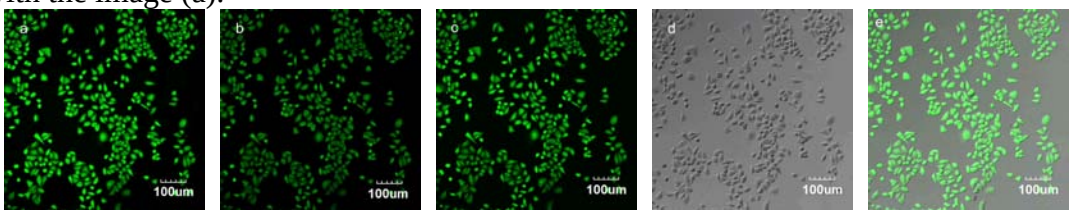

Figure S11. Confocal fluorescence images of redox changes in living HeLa cells. (a) Incubated FSeSeF for 5 min. (b) FSeSeF-loaded cells treated with 1 mM H_2O_2 for 20 min. (c) FSeSeF-loaded, H_2O_2-treated cells for treatment with 1 mM α-lipoic acid for 40 min. (d) Bright-field image of (c). (e) The overlay of (c) and (d). Images were acquired with an objective lens (×10) that in parallel to figure 3 (d)-(f). The excitation wavelength was 488 nm and emission range was from 495 to 595 nm. Scale bar represents 20 μm.

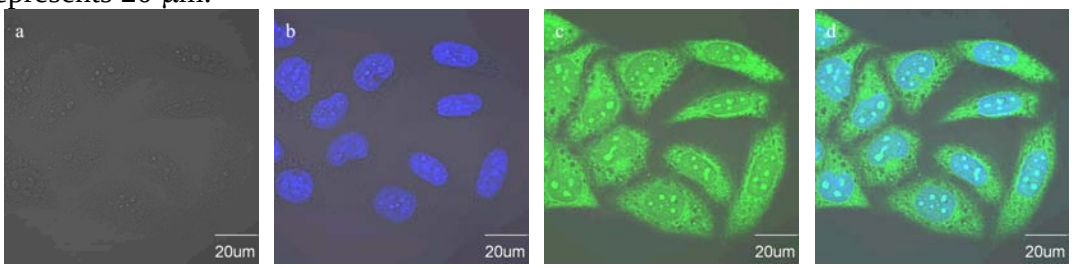

Figure S12. Bright-field images of Figure 3g–i. Image (b), (c), (d) was the overlay of Figure 3(h), (i), (j) with the image (a), respectively.

11. Additional Spectroscopic Data

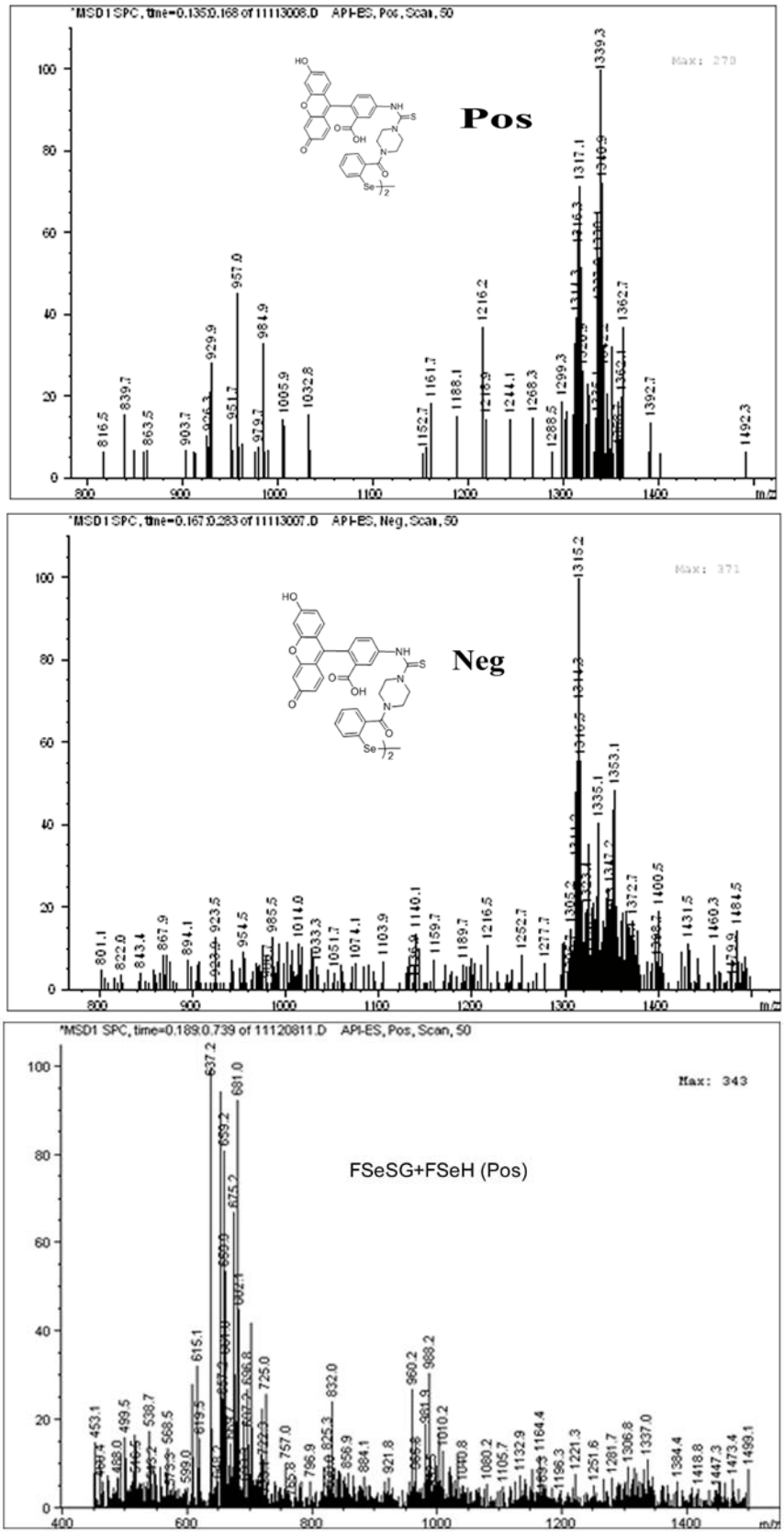

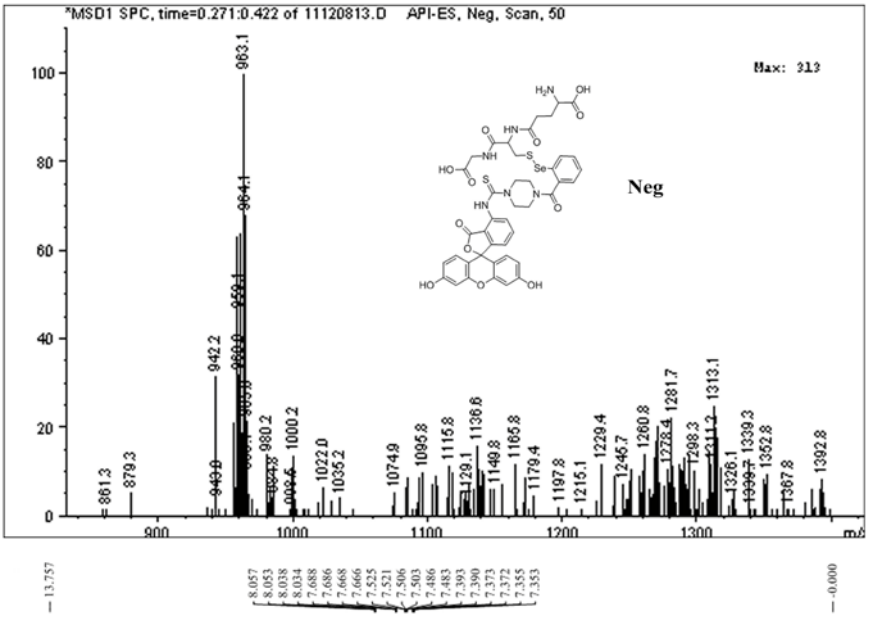

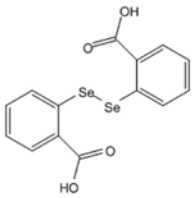

^{1}H NMR in $CDCl_3$

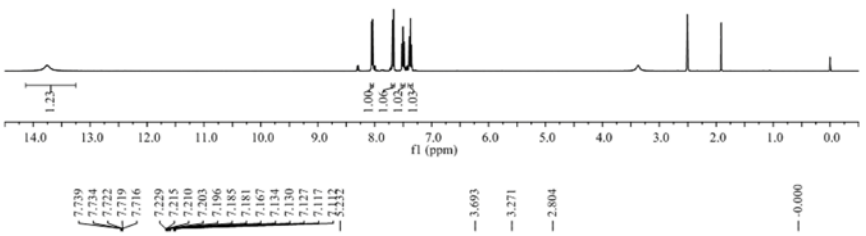

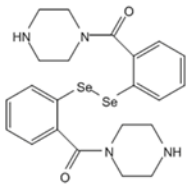

^{1}H NMR in $CDCl_3$

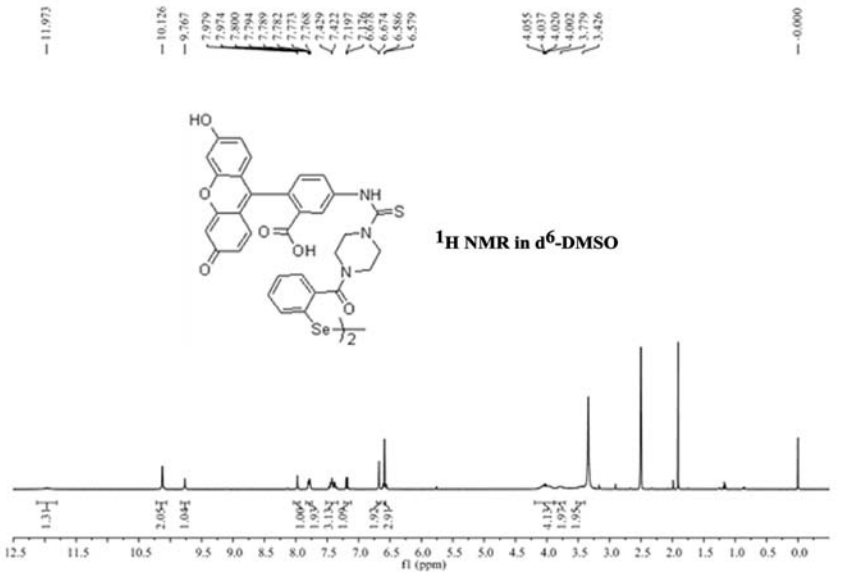
HO
NH
S
O
OH
N
Se
2
^{1}H NMR in d^{6}-DMSO
f1 (ppm)

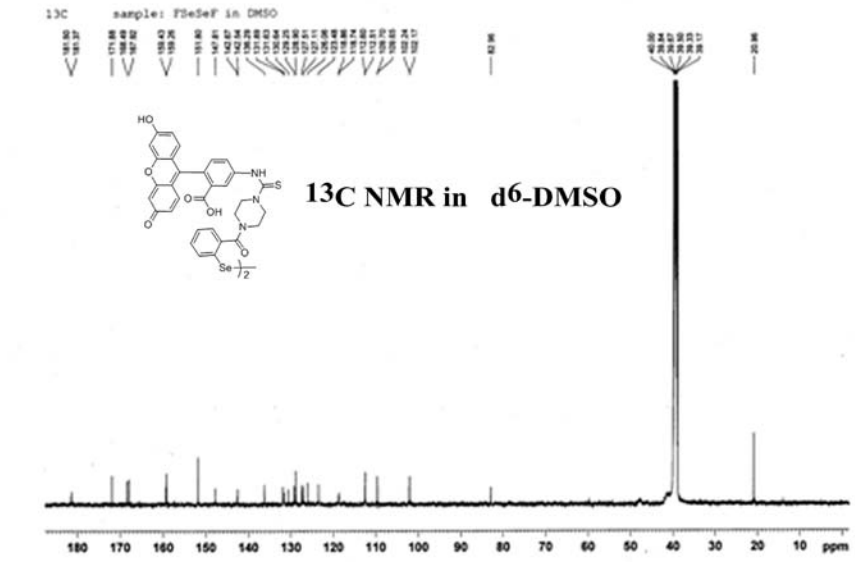
13C sample: FSeSeF in DMSO
^{13}C NMR in d^{6}-DMSO
ppm

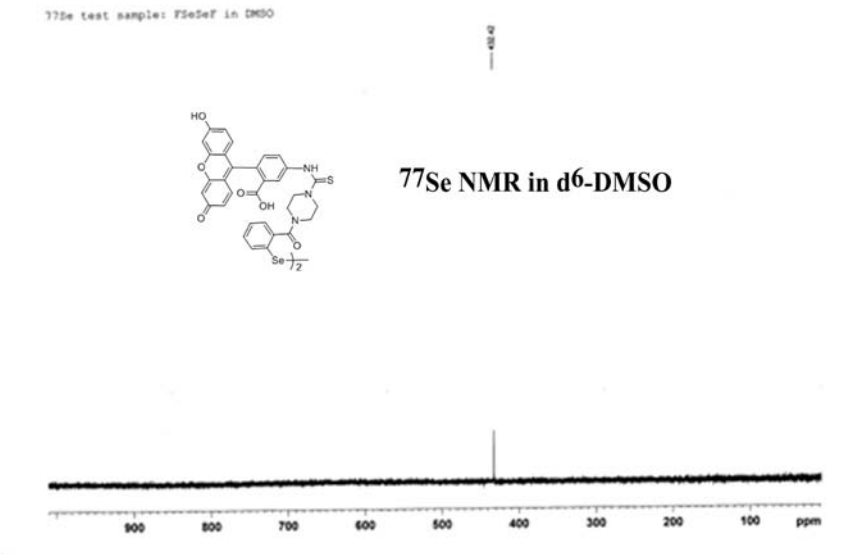
77Se test sample: FSeSeF in DMSO
^{77}Se NMR in d^{6}-DMSO
ppm

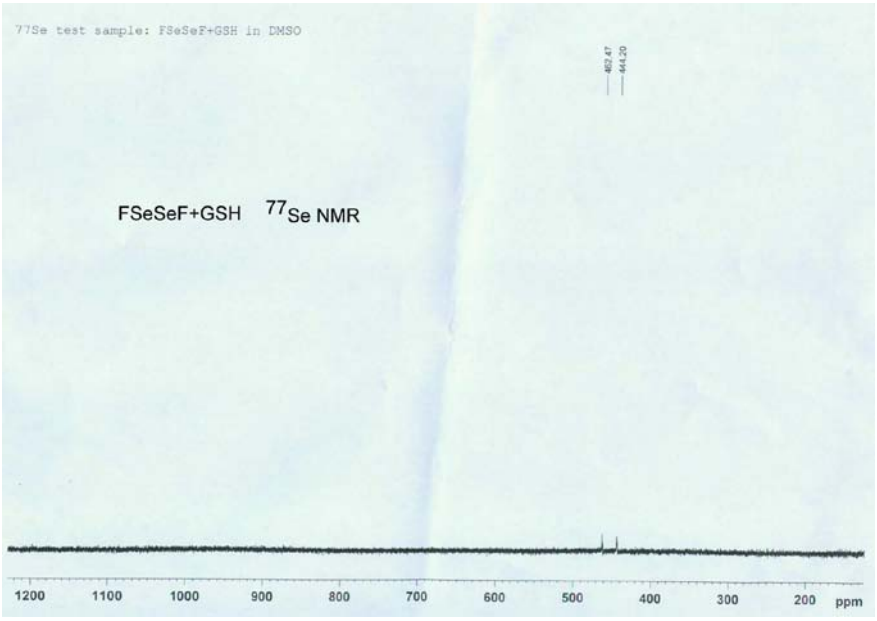

12. References

(1) Ashki, N.; Hayes, K. C.; Bao, F. *Neuroscience* 2008, **156**, 107-117.
(2) Free Radicals in Biology and Medicine. New York, Oxford University Press, 1989, 58-70.
(3) Albers A. E.; Okreglak V. S.; Chang C. J. *J. Am. Chem. Soc.*, 2006, **128**, 9640-9641.
(4) Halliwell B.; Gutteridge J. M. C.; *Arch. Biochem. Biophys.*, 1986, **246**, 501-514.
(5) Nieminen, A. L.; Byrne, A. M.; Herman B.; Lemasters, J. *Am. J. Physiol-Cell Ph.*, 1997, **272**, 1286-1294.
(6) Morris J. C. *J. Phys. Chem.*, 1966, **70**, 3798.
(7) Huber W. and Koella J. C., *Acta Trop.*, 1993, **55**, 257-261.
(9) D. L. Klayman; T. S. Griffin, *J. Am. Chem. Soc.*, 1973, **95**, 197.
(10)J. Mlochowski; R. J. Gryglewski; A. D. Inglot; A. Jakubowski; L. Juchniewicz; K. Kloc, *Liebigs Annalen* 1996, **0**, 1751.
(11) H. Wojtowicz; M. Chojnacka; J. Mlochowski; J. Palus; L. Syper; D. Hudecova; M. Uher; E. Piasecki; M. Rybka, *Farmaco (Lausanne)* 2003, **58**, 1235.
(12) M. Shortreed, R. Kopelman, M. Kuhn and B. Hoyland, *Anal. Chem.*, 1996, **68**, 1414-1418.
(13) G. M. Whitesides; J. E. Lilburn; R. P. Szajewski, *J. Org. Chem.*, 1977, **42**, 332.
(14) H. Maeda; H. Matsuno; M. Ushida; K. Katayama; K. Saeki; N. Itoh, *Angew. Chem. Int. Ed.*, 2005, **44**, 2922.
(15) L. Yi; H. Li,; L. Sun; L. Liu; C. Zhang; Z. Xi, *Angew. Chem. Int. Ed.*, 2009, **48**, 4034.